Nano Res
DOI 10.1007/s12274-012-0264-8
Research Article

ISSN 1998-0124
CN 11-5974/O4

Solution-Processed Flexible Transparent Conductors Composed of Silver Nanowire Networks Embedded in Indium Tin Oxide Nanoparticle Matrices

Choong-Heui Chung, Tze-Bin Song, Brion Bob, Rui Zhu, and Yang Yang (✉)

Department of Materials Science and Engineering and California NanoSystems Institute, University of California Los Angeles, Los Angeles, CA 90095, USA

Received: 19 August 2012 / Revised: 24 September 2012 / Accepted: 3 October 2012

ABSTRACT

Although silver nanowire meshes have already demonstrated sheet resistance and optical transmittance comparable to those of sputter-deposited indium tin oxide thin films, other critical issues including surface morphology, mechanical adhesion and flexibility have to be addressed before widely employing silver nanowire networks as transparent conductors in optoelectronic devices. Here, we demonstrate the efficacy of low temperature solution-processed flexible metal nanowire networks embedded in a conductive metal oxide nanoparticle matrix as transparent conductors, and investigate their microstructural, optoelectronic, and mechanical properties in attempting to resolve nearly all of the technological issues imposed on silver nanowire networks. Surrounding silver nanowires by conductive indium tin oxide nanoparticles offers low wire to wire junction resistance, smooth surface morphology, and excellent mechanical adhesion and flexibility while maintaining the high transmittance and the low sheet resistance. In addition, we discuss the relationship between sheet resistance and transmittance in the silver nanowire composite transparent conductors and their maximum achievable transmittance. Although we have selected silver nanowires and indium tin oxide nanoparticle matrix as demonstration materials, we anticipate that various metal nanowire meshes embedded in various conductive metal oxide nanoparticle matrices can effectively serve as transparent conductors for a wide variety of optoelectronic devices owing to their superior performance, simple, cost-effective, and gentle processing.

KEYWORDS

Transparent conductor, silver nanowire, conductive metal oxide nanoparticle, indium tin oxide

1. Introduction

Conducting metal oxides films such as indium tin oxide (ITO) films and aluminum doped zinc oxide films have been widely used as transparent conductors in a variety of optoelectronic devices including liquid crystal displays, touch screens, organic light emitting diodes, and thin film solar cells owing to their unique material properties capable of simultaneously demonstrating high optical transparency and high electrical conductivity. However, sputtering techniques are almost always required in order to properly deliver their favorable properties in the form of large area thin films [1–3]. The complexity of fabricating sputtered

Address correspondence to yangy@ucla.edu

films makes them less cost effective due to the use of vacuum equipment. To make matters worse, the brittle nature of sputtered ITO thin films makes its use difficult on flexible substrates because the films crack when the substrate is bent. Therefore, sputtered ITO thin films are not compatible with high-throughput roll to roll processing. Furthermore, when ITO films are sputter-deposited onto organic optoelectronic devices, energetic particles and heat generated during sputtering process can easily damage underlying organic layers leading to device degradation or failure [4–8]. Flexible transparent conductors processable under thermally and chemically benign conditions in non-vacuum environment are urgently needed to effectively replace sputtered ITO thin films for lower cost production and for emerging flexible electronics.

Calculations predict that metal nanowire networks have the potential to demonstrate substantially higher transmittance than sputtered ITO thin films at equivalent sheet resistance values [9]. In this approach, the high optical transmittance of the networks that can be achieved is not from their intrinsic optical properties but from the relatively low surface coverage of the nanowires. Therefore, in order to achieve comparable sheet resistance to that of sputtered ITO thin films at equivalent transmittance, nanowire materials have to have much higher intrinsic electrical conductivity than that of conductive metal oxides. Lee et al. first demonstrated that a solution-processed randomly dispersed silver nanowire (AgNW) mesh is a promising candidate to replace sputtered ITO thin films by providing both low sheet resistance and high transmittance [9]. However, in order for silver nanowire networks to be effectively incorporated into the wide range of modern optoelectronic devices, the following challenges must be simultaneously resolved: (1) wire to wire junction resistance; (2) surface roughness; (3) gaps between silver nanowires causing parasitic lateral current flow; (4) work function; (5) mechanical robustness including adhesion and flexibility; and (6) process compatibility [10].

Although significant progress regarding AgNW meshes has been achieved during the past five years in addressing the above issues by developing processing methods including mechanical pressing, thermal annealing, plasmonic welding, electrochemical gold coating, and layer transfer methods [11–26], all of the reported methods address only some of the above issues and their application is restricted to certain kinds of device structures. Therefore, new processing methods and materials structures must be further developed to simultaneously fulfill all of the above requirements. In addition, from a practical point of view, the fabrication and processing of materials should be simple and cost effective while maintaining excellent optoelectronic properties. Furthermore, low temperature processing in the preparation of silver nanowire networks will be desirable since it allows the use of heat sensitive flexible substrates.

In this work, we attempt to resolve nearly all of the current problems with AgNW networks by employing solution-deposition of conductive metal oxide nanoparticles onto pre-existing AgNW networks at low temperatures. Embedding the AgNW network in the conductive metal oxide nanoparticle matrix offers many advantages including improved wire to wire junction conductance, smooth surface morphology, excellent mechanical adhesion, and flexibility. As the first demonstration of this method, indium tin oxide nanoparticles (ITO-NP) were selected as the conductive metal oxide nanoparticles because of their relative maturity and industrial availability. Although our present electrode design contains indium, which suffers from concerns over supply and price, we expect that indium-free conductive metal oxide nanoparticles such as aluminum doped zinc oxide and antimony doped tin oxide nanoparticles may play equivalent roles to ITO-NP in future electrode architecture. We also believe that this electrode design will allow AgNW films to be practically employed in a wide range of optoelectronic device applications.

2. Experimental

AgNWs solutions (Seashell Technology, AgNW-115) were spun at spin speed of 1000 r/min for 60 s onto 165 μm-thick polyethylene terephthalate (PET) substrates to form a randomly dispersed AgNW network, and ITO-NP solution sequentially spun at a spin speed of 2000 r/min for 30 s onto the AgNW network followed by thermal annealing around 100 °C for a few minutes to remove the solvent. The AgNW solutions

were diluted to 1 mg/mL concentration. The AgNWs were approximately 115 nm in diameter and 30 μm in length. AgNW networks with different sheet resistance and optical transmittance values were obtained by repeated spin-coating processes. The employed ITO-NP solutions were prepared by mixing equal volumes of 30 wt.% of ITO-NPs dispersed in isopropyl alcohol (Sigma Aldrich) and 2.5 wt.% polyvinyl alcohol (PVA) dissolved in deionized water. The PVA solution was added to the ITO-NP dispersion to further improve mechanical adhesion of the resulting AgNW/ITO-NP films.

Scanning electron microscope (SEM) images were taken to investigate surface morphology and structural features of bare AgNW and AgNW/ITO-NP films. Atomic force microscopy (AFM) was used to characterize the surface roughness of the films. Optical specular transmittance of the films was measured using a Hitachi ultraviolet–visible spectrophotometer (U-4100) without an integrating sphere. Therefore, the measured transmittance values exclude Fresnel reflection and scattered light. A bare PET substrate was used as a reference in the transmittance measurements. The sheet resistances of the films were measured using the four-point probe method. The two-point probe method was used to measure the surface resistance of the films during bending test using a multimeter.

3. Results and discussion

3.1 Microstructure of AgNW/ITO-NP films

The surface morphology of a silver nanowire network is critically important to its successful incorporation into optoelectronic devices. The nature of randomly dispersed silver nanowire networks leads to protrusions produced by overlapping wires which are as approximately two or three times high as the diameter of the employed nanowires (Figs. 1(a) and 1(c)). This surface morphology is not suitable for the fabrication of modern thin film optoelectronic devices where the thickness of each layer is frequently less than 100 nm. This rough surface could frequently cause device short failure [18]. The subsequent deposition of ITO-NP film significantly improved the resulting surface roughness. The pre-deposited nanowire mesh was completely covered by ITO nanoparticles without leaving any gaps or space. As a result, the nanowires cannot be seen in the plane view SEM image (Fig. 1(b)). The localized height variation of the resulting film was the same order of magnitude as the size (10–30 nm) of the employed nanoparticles, as shown in the AFM scan (Fig. 2). The root mean square roughness and roughness average were 12.7 nm and 15.7 nm, respectively. These values are approximately one tenth of the local height

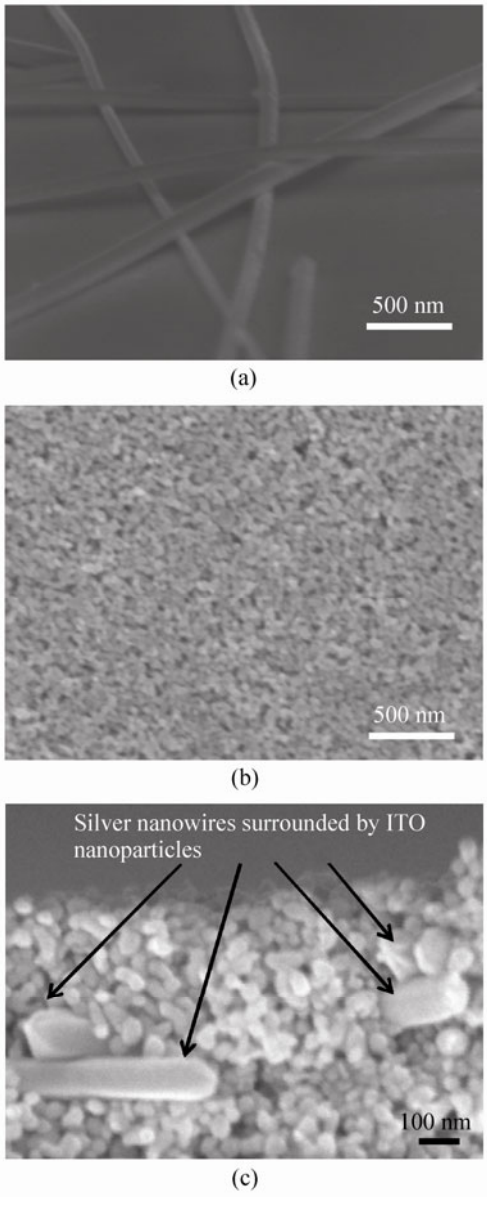

Figure 1 (a) Tilted (75°) view SEM images of a bare silver nanowire network. (b) Plain view SEM images of an indium tin oxide nanoparticle film deposited on pre-existing silver nanowire network. (c) Cross sectional SEM image of silver nanowire network embedded in an indium tin oxide nanoparticle matrix

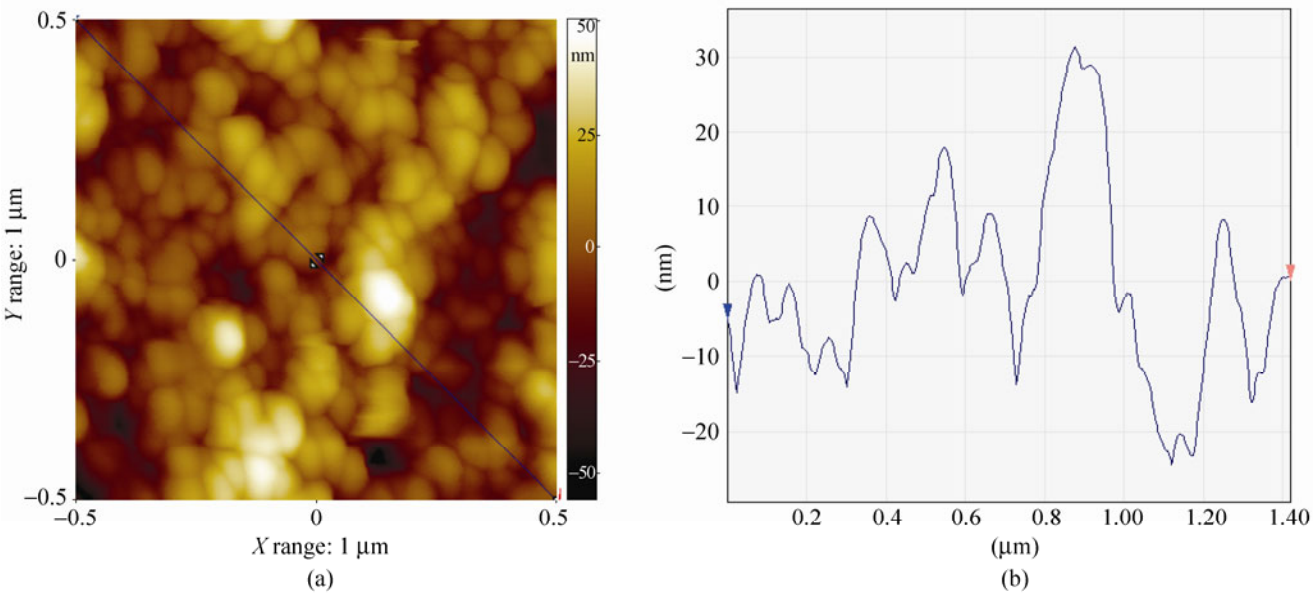

Figure 2 (a) AFM image of the AgNW/ITO-NP surface and (b) AFM height line profile of the surface

variation of bare AgNW films which can be 200–300 nm due to stacked wires in their junctions. It is expected that the surface roughness can be further improved by employing smaller sized nanoparticles.

The large lateral holes between silver nanowires are also seriously problematic in the lateral carrier collection of devices in which carrier diffusion length is not much larger than the gap size. This charge collection issue can be also solved owing to completely filling the holes present in the nanowire networks by transparent conductive material in optoelectronic devices [27]. Furthermore, the resulting surface of AgNW/ITO-NP will be favorable for building optoelectronic devices because most conventional thin film optoelectronic materials are optimized to be compatible with the electronic properties of the ITO surface.

3.2 Optoelectronic properties of AgNW/ITO-NP films

The sheet resistance of AgNW networks depends on the dimensions (length and diameter) of the wires, wire number density on the substrate surface, individual wire resistance, and wire to wire contact resistance. For a given dimension of the wires and wire number density, wire to wire junction resistance rather limits overall the sheet resistance due to its extremely high value, typically larger than 1 GΩ, in as-prepared AgNW networks [18]. It is thus critically important to ensure low wire to wire junction resistance. The possible existence of small vertical gaps between silver nanowires and insulating ligands used for synthesis and solution dispersion is likely to hinder carrier transport across the wire to wire junctions. Although fused wire to wire junctions can be readily achieved by thermal annealing around 180 ˚C or mechanical pressing, these methods may not be applicable for heat sensitive and/or readily deformable materials and devices.

The deposition of an ITO-NP matrix onto a bare AgNW network dramatically decreased the sheet resistance of the films (Fig. 3(a)). The sheet resistances of AgNW/ITO-NP films ranged from 0.01% to 18.9% of those of bare AgNW films, depending on the wire number density with a range of 0.3–1.6 μm^{-1} in the films (Fig. 3(b)). The meshes with smaller number density showed more significant decrease in sheet resistance. The decrease in sheet resistance cannot be explained by conduction taking place predominantly in the ITO nanoparticles because the sheet resistance of the plain ITO-NP film was as high as ~20 kΩ/□. Based on the observation that there was no obvious change of shape in the pre-deposited nanowire network after deposition of the ITO-NP matrix, these results thus verify the reduced wire to wire junction resistance after deposition of the conductive nanoparticle matrix.

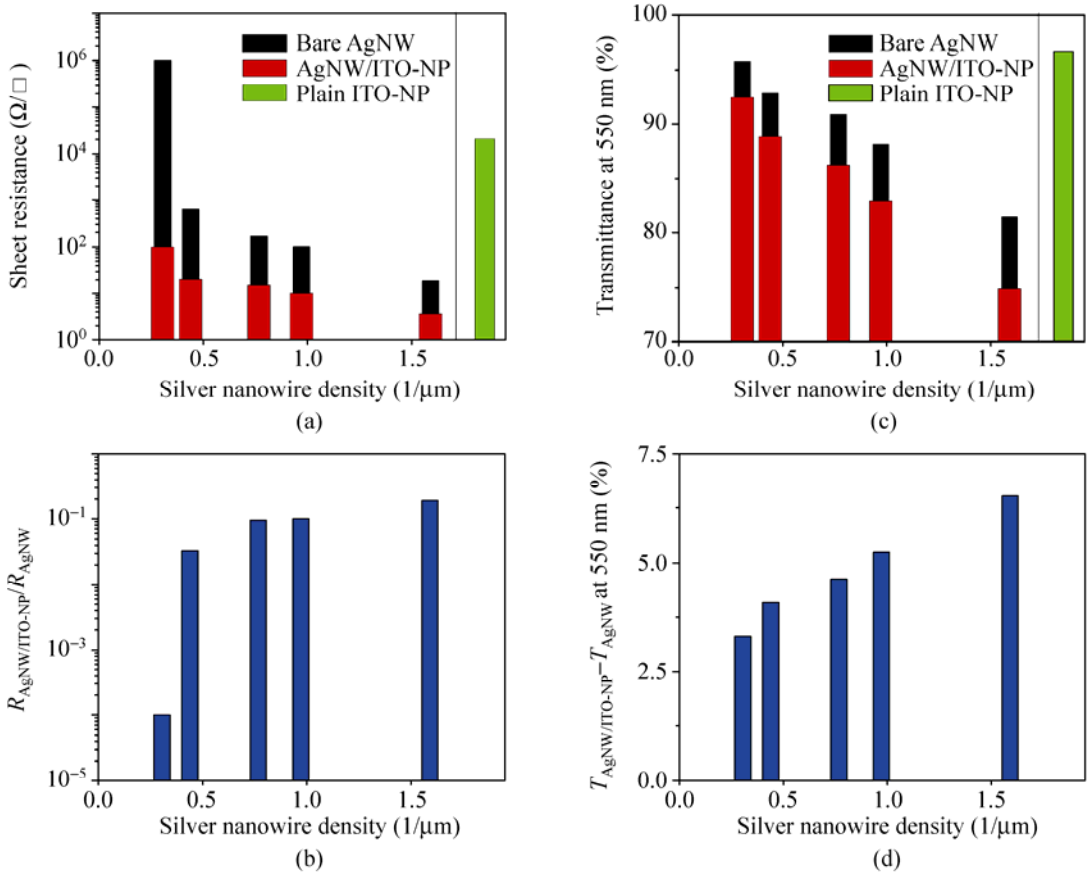

Figure 3 (a) Sheet resistance values of a plain indium tin oxide nanoparticle film and a number of silver nanowire networks before and after nanoparticle matrix deposition. (b) Ratios between the sheet resistance value of silver nanowire networks before and after the deposition of the indium tin oxide nanoparticle matrix. (c) Optical transmittance at 550 nm of a plain indium tin oxide nanoparticle film and a number of silver nanowire networks before and after the deposition of the indium tin oxide nanoparticle matrix. (d) Difference in the transmittance at 550 nm of the silver nanowire networks before and after deposition of the indium tin oxide nanoparticle matrix

The bare AgNW meshes with smaller wire number density have been shown to have larger average wire to wire junction resistance [9], which implies that the junction resistance is a more dominant component in the sheet resistance of the films with smaller wire number density. Thus, a more dramatic decrease in the sheet resistance of the films with smaller wire number density was observed because low wire to wire junction resistance was achieved in the all prepared networks by sequential deposition of the ITO-NP matrix.

The microstructure of the deposited AgNW/ITO-NP films supports the argument for improved wire to wire junction conductance. A cross-sectional SEM image shows that each AgNW is surrounded by densely packed ITO nanoparticles (Fig. 1(c)). The smaller size of the individual ITO nanoparticles relative to the dimensions of the AgNWs likely allows them to readily pack into the gaps left in the as-deposited mesh. The reduction of wire to wire contact resistance can thus be attributed to the conductive ITO nanoparticles filling the vertical gaps which allows the wires to become connected together via a conductive medium. Free electrons are then able to flow across wire to wire junction without undergoing significant electrical resistance.

High optical transmittance is as important as low sheet resistance in transparent conductors. The transmittance of the AgNW films was only slightly decreased by 3.3% to 6.5% after ITO-NP matrix deposition, depending on wire number density in the range 0.3–1.6 μm^{-1} (Figs. 3(c) and 3(d)) while a significant decrease was simultaneously observed in

the sheet resistance of the films. The films with higher wire number density showed more transmittance loss after deposition of the ITO-NP matrix. Considering ITO-NP films showed a transmittance of 96.7% at 550 nm, and the measured specular transmittance excluded scattered light, it is likely that the optical transmittance losses of more than 3.3% after deposition of the ITO-NP film onto existing AgNW films is associated with the enhanced light scattering in the AgNW/ITO-NP. The enhanced scattered light could be advantageous for thin film photovoltaic devices by providing better absorption of light in absorber layers and better photogenerated carrier collection. The enhanced light scattering by silver nanowire based electrodes has been reported to improve the short circuit current density in organic and inorganic thin film solar cells [9, 27]. Organic solar cells would perhaps be expected to benefit most from this effect. These organic devices are often unable to completely absorb light because their absorber layer thickness is typically limited by short carrier diffusion lengths. Enhanced light scattering could be also useful to reduce the thickness of absorber layers in chalcogenides and polycrystalline or amorphous silicon solar cells.

The transmittance values of AgNW/ITO-NP films with several different sheet resistance values are shown in Fig. 4(a). The transmittance at 550 nm reached 90.5% when the sheet resistance was 44 Ω/□; 88.6% at 23 Ω/□, and 85.3% at 11 Ω/□. The transmittance of the films was essentially constant across all measured wavelength regions because optical transmittance in metal nanowire films is controlled almost entirely by the sparseness of the metal wire network. Our low temperature solution-deposited AgNW networks embedded in ITO-NP matrices showed sheet resistance and transmittance values comparable to commercially available sputtered-deposited ITO electrodes as well as the reported values for AgNW networks and AgNW composites [17–22, 25, 26] (Fig. 4(b)).

3.3 Percolation in AgNW/ITO-NP films

Predicting the relationship between transmittance and sheet resistance will be useful because these two parameters are perhaps the most important properties in the selection of effective transparent conductors. Percolation theory for randomly dispersed one-dimensional objects predicts the relationship between the sheet resistance and the wire areal number density as below [28]

$$1/R_S \propto (N - N_C)^{\alpha} \text{ and } N_C = 17.94/\pi L^2 \quad (1)$$

where R_S is the sheet resistance of the networks, N is the wire areal number density dispersed on the surface, N_C is wire areal number density at the threshold point, L is the wire length, and α is an exponent depending on the dimension of the resulting meshes.

To relate the sheet resistance to the transmittance from the above percolation theory, we need the relationship between the transmittance and the wire

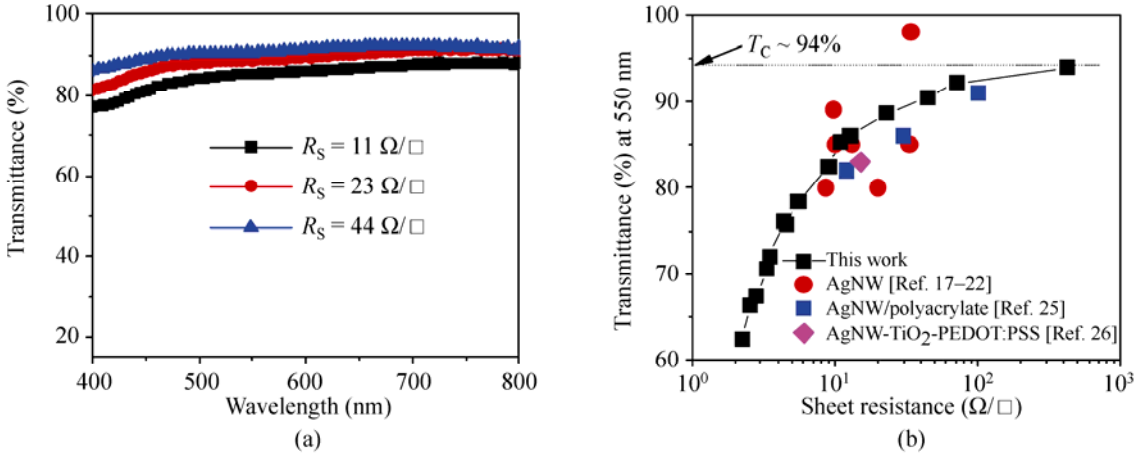

Figure 4 (a) Variation in transmittance of the AgNW/ITO-NP films with wavelength for three different sheet resistance values. (b) Plot of transmittance versus sheet resistance, the maximum achievable transmittance of conductive AgNW/ITO-NP films, and the literature values for AgNW and AgNW composites

areal number density. The surface coverage (SC) will be the average projected area of wires (*LD*) multiplied by the wire areal number density (*N*) as below

$$\mathrm{SC} = LD \times N \tag{2}$$

where *D* is the diameter of the metal wires. The transmittance loss in metal nanowire networks is mainly due to the reflective scattering of light by the metal nanowires. The loss of optical transmittance of the bare AgNW will be thus approximately equal to the surface coverage of the metal nanowires, and the transmittance can be described as below

$$T = 100 \times (1 - \mathrm{SC})\% = 100 \times (1 - LDN)\% \tag{3}$$

At the percolation point

$$\begin{aligned} \mathrm{SC}_\mathrm{C} &= N_\mathrm{C} \times LD = 17.94LD/\pi L^2 = 5.71D/L \\ T_\mathrm{C} &= 100 \times (1 - 5.71D/L)\% \end{aligned} \tag{4}$$

Thus, the transmittance at the percolation point, T_C, equivalent to achievable maximum transmittance of a conductive network, is solely determined by the aspect ratio of the wires while the critical wire areal number density is solely determined by the length of wires. The nanowires employed in this work have approximate diameters of 115 nm and lengths of around 30 μm. T_C is thus estimated to be approximately 97.8%.

To validate our assumption that the loss of optical transmittance of AgNW networks is approximately equal to the surface coverage of the metal nanowires, we plotted the variation in transmittance loss (100–*T*) (%) for the AgNW networks as a function of the surface coverage of silver nanowires both before and after ITO-NP deposition. Figures 5(a)–5(e) show plane view SEM images of bare AgNW films with different number densities of silver nanowires with values ranging from 0.305 to 1.59 μm^{-1}. The surface coverage is estimated by multiplying the diameter (115 nm) of the wires and the wire number density measured from the SEM images of the AgNW networks before the ITO-NP deposition. The surface coverage is nearly equal to the transmittance loss of the bare AgNW, which validates

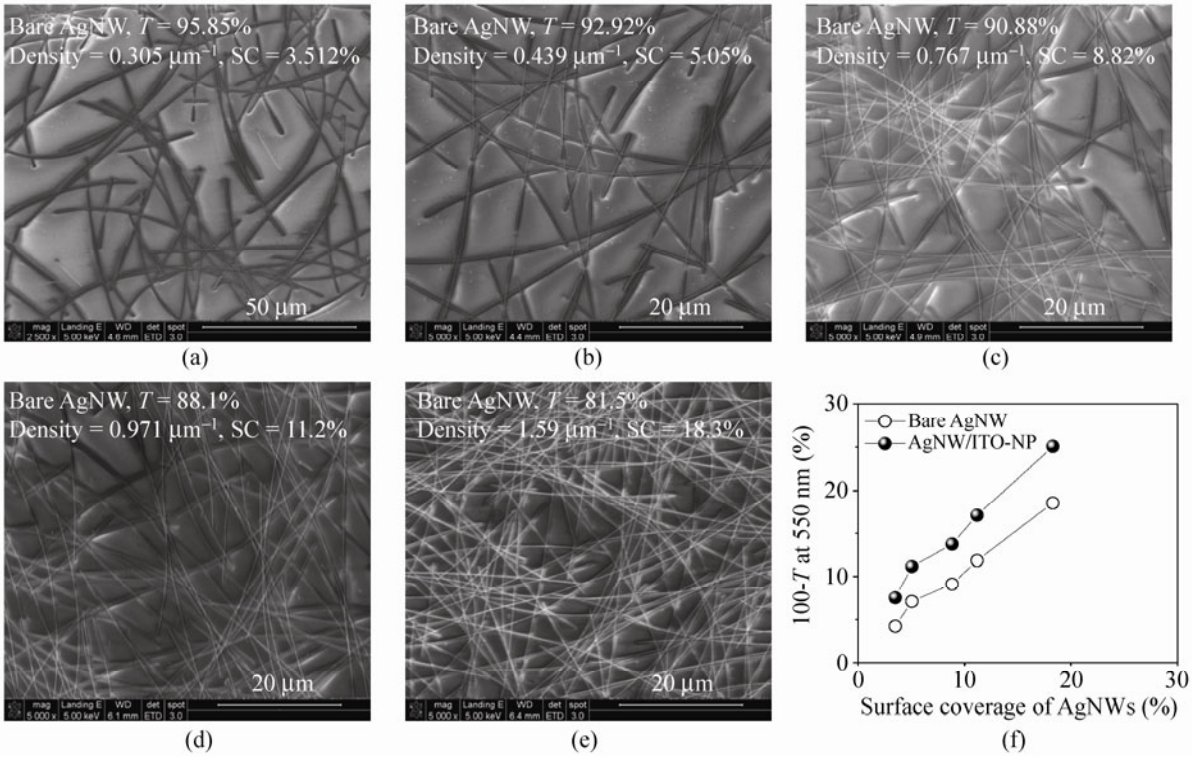

Figure 5 Plane view SEM images of bare AgNW networks with a nanowire density of (a) 0.305 μm^{-1}, (b) 0.439 μm^{-1}, (c) 0.767 μm^{-1}, (d) 0.972 μm^{-1}, (e) 1.59 μm^{-1}. (f) Optical transmission loss (100–*T*) of bare AgNW and AgNW/ITO-NP films as a function of the surface coverage of silver nanowires

our assumption (Fig. 5(f)). The maximum transmittance of the transparent AgNW/ITO-NP was determined to be 94% from the plot of the sheet resistance versus the transmittance (Fig. 4(b)**)** which is 3.8% lower than the calculated value of 97.8%. This difference results from additional transmittance loss by large angle light scattering and light absorption by the ITO-NP matrix.

By combining equations (1)–(4), the variation in sheet resistance, R_S as a function of optical transmittance, T, can be described by the equation

$$1/R_S \propto (T_C - T)^{\alpha} \quad (5)$$

The linear plot of log (R_S) vs. log (T_C–T) allows us to extract α values of 1.46 and 1.27 at 550 nm and 600 nm, respectively (Fig. 6). These values are similar to the theoretical value of $\alpha = 1.33$ for the relationship between nanowire number density and surface conductance in two-dimensional networks [28], and also similar to the reported values of 1.42 experimentally determined from the relationship between amount of nanowire deposited on the substrate surface and the surface conductance of nanowire films [20].

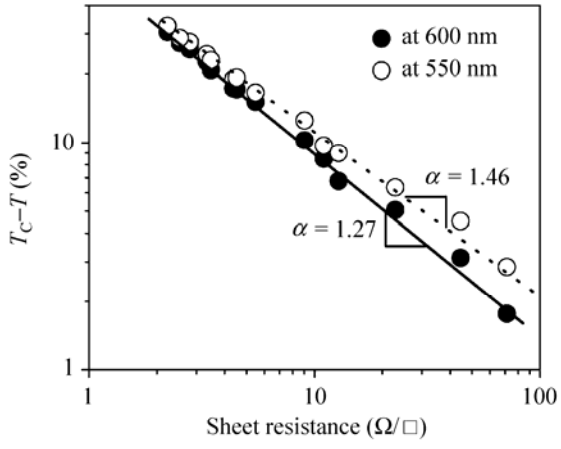

Figure 6 The linear plot of log (R_S) vs log (T_C–T) allows us to extract α values of 1.46 and 1.27 at 550 nm and 600 nm, respectively, from the equation: $1/R_S \propto (T_C - T)^{\alpha}$

3.4 Mechanical properties of AgNW/ITO-NP films

In order for a potential electrode material to be used in flexible devices and to be compatible with roll to roll processing, the electrode must meet certain mechanical requirements including adhesion and flexibility. Tape tests were executed in the regions shown by the dotted lines in Fig. 7 to test the adhesion of the AgNW film to the substrate. 3M tape (Scotch® Magic™ Tape) was pressed with a pressure of an approximately 2 MPa for 30 s. As described in the experimental section, we mixed a PVA solution with the as-purchased ITO-NP solution to prepare the final ITO-NP solution in order to achieve improved film adhesion. The addition of the PVA dramatically improved the film adhesion without sacrificing transmission or sheet resistance. While bare AgNW films were completely peeled off during the tape test, the nanocomposite remained on the substrate without any change in transmittance or sheet resistance, demonstrating the excellent mechanical adhesion of the AgNW/ITO-NP film. In addition to mechanical adhesion, the AgNW/ITO-NP offers excellent mechanical flexibility even under severe concave and convex bending (Fig. 8(a)). The surface resistance of the AgNW/ITO-NP film was observed to change by approximately 30% of its initial value when the film was bent to a 0.5 cm radius of curvature. For convex (concave) bending, the surface resistance of the film decreased (increased) with decreasing radius of curvature. It is likely that convex bending of the substrate induces compressive forces at the wire to wire junction, which in turn may improve the wire to wire junction conductance. This indicates that AgNW networks embedded in ITO-NP matrices have further room for improvement. More importantly, the resistance completely recovered its original value

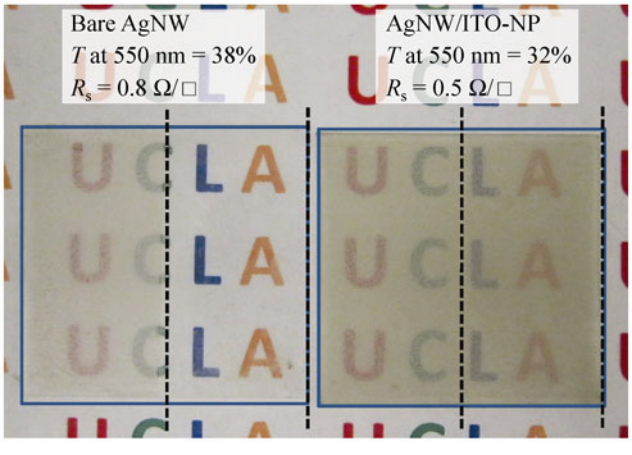

Figure 7 Photos of bare AgNW and AgNW/ITO-NP films after tape tests. The tape test was executed for the regions shown by the dotted lines in the photos to test the adhesion of the AgNW film to the substrate

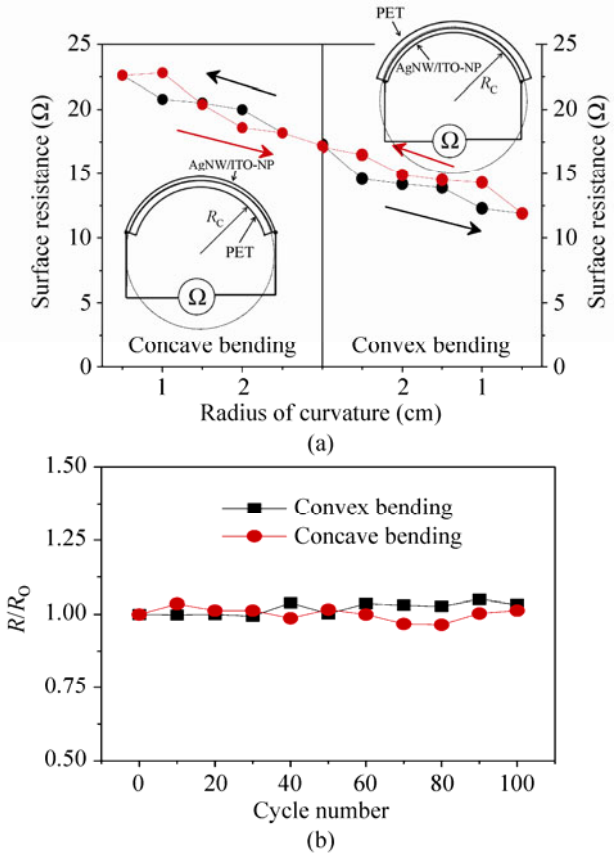

Figure 8 (a) Variation in the surface resistance of the AgNW/ITO-NP film deposited on a PET substrate as a function of radius of curvatures (R_C) in concave and convex bending. (b) Variations in the final surface resistance of an AgNW film as a function of number of cycles of bending to a 0.5 cm radius of curvature in concave and convex bending. The resistance values were measured after the substrate was relaxed to back to planar shape

when the substrate was relaxed to back to a planar shape even after as many as one hundred bending cycles to a radius of curvature of 0.5 cm (Fig. 8(b)). This recovery is attributed to the flexible nanoparticle matrix firmly holding nanowire network in place, which prevents the permanent deformation of the networks.

4. Conclusions and Prospects

Low temperature solution-deposited AgNW networks embedded in ITO-NP matrices demonstrate significant improvement in surface morphology, mechanical adhesion, and flexibility while maintaining the sheet resistance and transmittance values necessary to replace conventional sputtered ITO thin films. Surrounding the AgNW network by ITO has been observed to dramatically improve wire to wire conductance. The improved surface morphology is achieved by completely filling the gaps left between nanowires and fully covering the nanowires with nanoparticles. Anchoring the nanowire network in place using a nanoparticle matrix also offers excellent substrate adhesion and mechanical flexibility. We expect that electrode structures involving metal nanowire networks embedded in conductive metal oxide nanoparticle matrices can be successfully incorporated into a variety of device structures suitable for a diverse set of applications.

References

[1] Ishibashi, S.; Higuchi, Y.; Ota, Y.; Nakamura, K. Low resistivity indium–tin oxide transparent conductive films. I. Effect of introducing H_2O gas or H_2 gas during direct current magnetron sputtering. *J. Vac. Sci. Technol. A* **1990**, *8*, 1399–1402.

[2] Ishibashi, S.; Higuchi, Y.; Ota, Y.; Nakamura, K. Low resistivity indium–tin oxide transparent conductive films. II. Effect of sputtering voltage on electrical property of films. *J. Vac. Sci. Technol. A* **1990**, *8*, 1403–1406.

[3] Carcia, P. F.; McLean, R. S.; Reilly, M. H.; Li, Z. G.; Pillione, L. J.; Messier, R. F. Low-stress indium–tin–oxide thin films rf magnetron sputtered on polyester substrates. *Appl. Phys. Lett.* **2002,** *81*, 1800–1802.

[4] Gu, G.; Bulovic, V.; Burrows, P. E.; Forrest, S. R.; Thompson, M. E. Transparent organic light emitting devices. *Appl. Phys. Lett.* **1996**, *68*, 2606–2608.

[5] Burrows, P. E.; Gu, G.; Forrest, S. R.; Vicenzi, E. P.; Zhou, T. X. Semitransparent cathodes for organic light emitting devices. *J. Appl. Phys.* **2000**, *87*, 3080–3085.

[6] Suzuki, H.; Hikita, M. Organic light-emitting diodes with radio frequency sputter-deposited electron injecting electrodes. *Appl. Phys. Lett.* **1996**, *68*, 2276–2278.

[7] Chung, C. H.; Ko, Y. W.; Kim, Y. H.; Sohn, C. Y.; Chu, H. Y.; Lee, J. H. Improvement in performance of transparent organic light-emitting diodes with increasing sputtering power in the deposition of indium tin oxide cathode. *Appl. Phys. Lett.*, **2005**, *86*, 093504.

[8] Chung, C. H.; Ko, Y. W.; Kim, Y. H.; Sohn, C. Y.; Chu, H. Y.; Park, S. H. K.; Lee, J. H. Radio frequency magnetron sputter-deposited indium tin oxide for use as a cathode in transparent organic light-emitting diode. *Thin Solid Films*

2005, *491*, 294–297.

[9] Lee, J. Y.; Connor, S. T.; Cui, Y.; Peumans, P. Solution processed metal nanowire mesh transparent electrodes. *Nano Lett.* **2008**, *8*, 689–692.

[10] Hu, L. B.; Wu, H.; Cui, Y. Metal nanogrids, nanowires, and nanofibers for transparent electrodes. *MRS Bull.* **2011**, *36*, 760–765.

[11] Lee, J. Y.; Connor, S. T.; Cui, Y.; Peumans, P. Semitransparent organic photovoltaic cells with laminated top electrode. *Nano Lett.* **2010**, *10*, 1276–1279.

[12] Gaynor, W.; Lee, J. Y.; Peumans, P. Fully solution-processed inverted polymer solar cells with laminated nanowire electrodes. *ACS Nano* **2010**, *4*, 30–34.

[13] Liu, C. H.; Yu, X. Silver nanowire-based transparent, flexible, and conductive thin film. *Nanoscale Res. Lett.* **2011**, *6*, 75.

[14] Yang, L. Q.; Zhang, T.; Zhou, H. X.; Price, S. C.; Wiley, B. J.; You, W. Solution-processed flexible polymer solar cells with silver nanowire electrodes. *ACS Appl. Mater. Interfaces*, **2011**, *3*, 4075–4084.

[15] Garnett, E. C.; Cai, W. S.; Cha, J. J.; Mahmood, F.; Connor, S. T.; Christoforo, M. G.; Cui, Y.; McGehee, M. D.; Brongersma, M. L. Self-limited plasmonic welding of silver nanowire junctions. *Nat. Mater.* **2012**, *11*, 241–249.

[16] Lu, Y. C.; Chou, K. S. Tailoring of silver wires and their performance as transparent conductive coatings. *Nanotechnology* **2010**, *21*, 215707.

[17] De, S.; Higgins, T. M.; Lyons, P. E.; Doherty, E. M.; Nirmalraj, P. N.; Blau, W. J.; Boland, J. J.; Coleman, J. N. Silver nanowire networks as flexible, transparent, conducting films: Extremely high DC to optical conductivity ratios. *ACS Nano* **2009**, *3*, 1767–1774.

[18] Hu, L. B.; Kim, H. S.; Lee, J. Y.; Peumans, P.; Cui, Y. Scalable coating and properties of transparent, flexible, silver nanowire electrodes. *ACS Nano* **2010**, *4*, 2955–2963.

[19] Madaria, A. R.; Kumar, A.; Zhou, C. W. Large scale, highly conductive and patterned transparent films of silver nanowires on arbitrary substrates and their application in touch screens. *Nanotechnology* **2011**, *22*, 245201.

[20] Madaria, A. R.; Kumar, A.; Ishikawa, F. N.; Zhou, C. W. Uniform, highly conductive, and patterned transparent films of a percolating silver nanowire network on rigid and flexible substrates using a dry transfer technique. *Nano Res.* **2010**, *3*, 564–573.

[21] Tokuno, T.; Nogi, M.; Karakawa, M.; Jiu, J.; Nge, T. T.; Aso, Y.; Suganuma, K. Fabrication of silver nanowire transparent electrodes at room temperature. *Nano Res.* **2011**, *4*, 1215–1222.

[22] Leem, D. S.; Edwards, A.; Faist, M.; Nelson, J.; Bradley, D. D. C.; de Mello, J. C. Efficient organic solar cells with solution-processed silver nanowire electrodes. *Adv. Mater.* **2011**, *23*, 4371–4375.

[23] Zeng, X. Y.; Zhang, Q. K.; Yu, R. M.; Lu, C. Z. A new transparent conductor: Silver nanowire film buried at the surface of a transparent polymer. *Adv. Mater.* **2010**, *22*, 4484–4488.

[24] Gaynor, W.; Burkhard, G. F.; McGehee, M. D.; Peumans, P. Smooth nanowire/polymer composite transparent electrodes. *Adv. Mater.* **2011**, *23*, 2905–2910.

[25] Yu, Z. B.; Zhang, Q. W.; Li, L.; Chen, Q.; Niu, X. F.; Liu, J.; Pei, Q. B. Highly flexible silver nanowire electrodes for shape-memory polymer light-emitting diodes. *Adv. Mater.* **2011**, *23*, 664–668.

[26] Zhu, R.; Chung, C. H.; Cha, K. C.; Yang, W. B.; Zheng, Y. B.; Zhou, H. P.; Song, T. B.; Chen, C. C.; Weiss. P. S.; Li, G.; Yang, Y. Fused silver nanowires with metal oxide nanoparticles and organic polymers for highly transparent conductors. *ACS Nano* **2011**, *5*, 9877–9882.

[27] Chung, C. H.; Song, T. B.; Bob, B.; Zhu, R.; Duan, H. S.; Yang, Y. Silver nanowire composite window layers for fully solution-deposited thin film photovoltaic devices. *Adv. Mater.* **2012**, *24*, 5499–5504.

[28] Hu, L.; Hecht, D. S.; Gruner, G. Percolation in transparent and conducting carbon nanotube networks. *Nano Lett.* **2004**, *4*, 2513–2517.